Synthesis and Self-Assembly of Polymer-Coated Ferromagnetic Nanoparticles

Pei Yuin Keng,[†] Inbo Shim,[†,‡] Bryan D. Korth,[†] Jack F. Douglas,[§] and Jeffrey Pyun[†,*]

[†]Department of Chemistry, University of Arizona, Tucson, Arizona 85721, [‡]Department of Nano and Electronic Physics, Kookmin University, Seoul, Korea 136-702, and [§]Polymers Division, National Institute of Standards and Technology, Gaithersburg, Maryland 20899

ABSTRACT We describe the synthesis and characterization of polymer-coated ferromagnetic cobalt nanoparticles (CoNPs). The synthesis of end-functionalized polystyrene surfactants possessing amine, carboxylic acid, or phosphine oxide end-groups was accomplished using atom-transfer radical polymerization. This versatile synthetic method enabled the production of multigram quantities of these polymeric surfactants that stabilized ferromagnetic CoNPs when dispersed in organic media. An in-depth investigation into the synthesis of polystyrene-coated ferromagnetic CoNPs was also conducted using various combinations of these polymeric surfactants in the thermolysis of dicobaltoctacarbonyl ($Co_2(CO)_8$). Moreover, the application of a dual-stage thermolysis with $Co_2(CO)_8$ allowed for the preparation of large samples (200–820 mg) per batch of well-defined and dispersable ferromagnetic nanoparticles. Characterization of these functionalized nanoparticle materials was then done using transmission electron microscopy, X-ray diffraction, vibrating sample magnetometry, and thermogravimetric analysis. Self-assembly of these dipolar nanoparticles was investigated in solutions cast onto supporting substrates, where local nematic-like ordering of nanoparticle chains was observed along with a tendency of adjacent chains to form "zippering" configurations, both phenomena having been predicted by recent simulations of dipolar fluids in conjunction with van der Waals interactions.

KEYWORDS: magnetic nanoparticles · magnetic nanocomposites · nanoparticle assembly · self-assembly · equilibrium polymerization · ring formation · polymer stabilization · particle synthesis · particle characterization

The use of dipolar nanoparticles (NPs) as building blocks to prepare organized hierarchical materials is an emerging area of great potential in materials chemistry. Ferromagnetic colloids are of interest for this application, as the inherent dipole moment of these materials enables one- and two-dimensional assembly into novel mesostructures.[1–8] Numerous previous reports have demonstrated the formation of magnetic assemblies from both ferromagnetic and superparamagnetic NPs on supporting surfaces to form 1-D chains,[9–16] flux closure rings,[17–19] 2-D superlattices of closed packed nanocrystals,[3,20–26] and 3-D labyrinth-like suprastructures.[27–33] Additionally, organized assemblies of magnetic nanoparticle building blocks have also been directly observed in solution using cryogenic electron microscopy[34–37] and atomic force microscopy of assemblies at cross-linkable oil–water interfaces.[38,39] One of the basic challenges of studying and utilizing these materials is obtaining appreciable quantities of ferromagnetic NPs possessing uniform size and well-defined magnetic properties. Additionally, these ferromagnetic NPs should also possess tunable surface chemistry and robust capping ligands that enable facile redispersion of isolated nanoparticle powders into common organic solvents after storage in air. Recent advances achieved in the solution synthesis of monodisperse magnetic NPs have enabled compositional control for the preparation of metallic, metal oxide, or bimetallic alloys using small-molecule surfactants.[40,41]

In addition to small-molecule surfactants, the preparation of organic–inorganic magnetic nanocomposites that possess polymer shells and magnetic nanoparticle cores has also been conducted.[42–44] This approach is particularly attractive since the modular nature of polymeric materials enables the synthesis of a wide range of hybrid nanocomposites.[45–48] Pre-synthesized magnetic NPs (Fe, Co, Fe_2O_3, Fe_3O_4) have also been decorated with various functional macromolecules, such as poly(ethylene glycol),[49–53] polyamidoamine dendrimers,[54] and cross-linkable polymer shells,[55,56] to impart water solubility, controlled interparticle spacing, and colloidal stability, respectively. Alternatively, surface-initiated polymerization has been employed to graft well-defined (co)polymers onto superparamagnetic NPs, making it possible to tune film thickness, composition, and mechanical properties.[57–67]

Polymer-coated ferromagnetic cobalt nanoparticles (CoNPs) have been synthesized by the thermolysis of metal–carbonyl precursors ($Co_2(CO)_8$, $Fe(CO)_5$) both in the presence of functional polymeric

*Address correspondence to jpyun@email.arizona.edu.

Received for review July 27, 2007 and accepted October 05, 2007.

Published online November 30, 2007.
10.1021/nn7001213 CCC: $37.00

© 2007 American Chemical Society

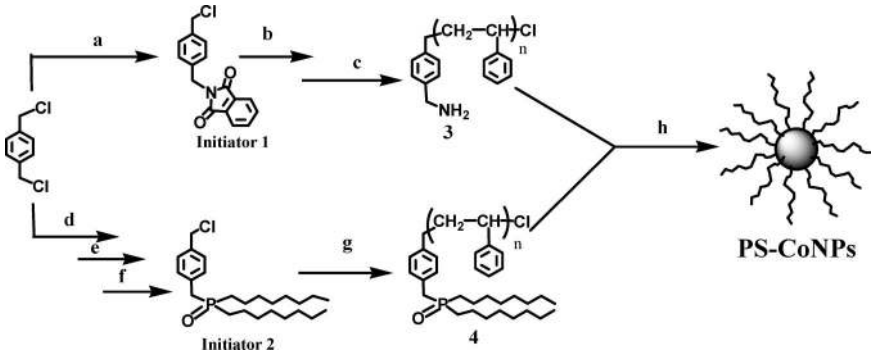

Scheme 1. Synthesis of ferromagnetic PS-CoNPs *via* thermolysis of $Co_2(CO)_8$ using a dual-stage temperature process at 175 and 160 °C, using PS-NH_2 (3) and PS-DOPO (4) surfactants. Synthesis of polymeric surfactants 3 and 4 was conducted by the ATRP of styrene using functional initiators 1 and 2, respectively. Conditions: (a) potassium phthalimide, CH_3CN, 80 °C; (b) styrene, CuCl, 2,2′-bipyridine, DMF, 110 °C; (c) NH_2NH_2, THF, MeOH, 25 °C; (d) $NaOCH_3$, MeOH, THF, 25 °C; (e) DOPO, NaH, THF, 65 °C; (f) BCl_3, CH_2Cl_2, 0 °C; (g) styrene, CuCl, 4,4′-dinonyl-2,2′-bipyridine, 110 °C; (h) thermolysis of the $Co_2(CO)_8$ at 175 °C, followed by growth at 160 °C for 30 min.

surfactants, such as random copolymers containing polar groups,[10,12,68] and within block copolymer templates.[69–73] Stöver and co-workers have also demonstrated the preparation of polymer-coated iron nanoparticles in multigram quantities.[44] However, a simple preparation of uniform and well-defined polymer-coated ferromagnetic CoNPs in appreciable quantities has not been reported. On the basis of the pioneering work of Thomas[10] and Alivisatos,[74,75] our group expanded upon these synthetic methodologies by preparing well-defined end-functional polystyrene surfactants bearing either amine or phosphine oxide ligating moieties to mediate the growth of ferromagnetic polystyrene-coated cobalt nanoparticles (PS-CoNPs).[76] This approach is attractive as the characteristics of polymers and small-molecule surfactants are combined, enabling the preparation of uniform ferromagnetic colloids that assemble into 1-D mesoscopic chains. In our previous report, functional alkoxyamine initiators were synthesized for nitroxide-mediated polymerization (NMP)[77,78] to prepare end-functional polystyrene surfactants of precise molar mass and composition. However, this approach was not amenable to synthesize large quantities of PS-CoNPs due to the multistep synthesis required for functional alkoxyamine initiators.

Herein, we report a simplified synthesis of uniform ferromagnetic PS-CoNPs from the thermolysis of dicobaltoctacarbonyl ($Co_2(CO)_8$) using end-functional polystyrene surfactants prepared using atom-transfer radical polymerization (ATRP).[79] The use of ATRP to prepare polystyrene surfactants afforded a facile route to these materials using commercially available starting materials, or precursors that were readily prepared with a minimal number of synthetic steps. Furthermore, we report on our mechanistic investigation into the preparation of PS-CoNPs using various polymeric surfactants. During the course of this effort, a facile method to synthesize PS-CoNPs in nearly 1-g batches was developed that answered the need of sample production as previously discussed. The experimental observation of a novel dipolar assembled morphology using these ferromagnetic PS-CoNPs is also reported.

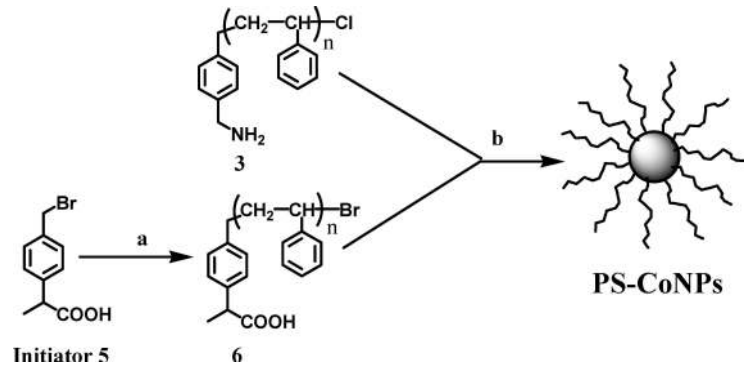

Scheme 2. Synthesis of ferromagnetic PS-CoNPs *via* thermolysis of $Co_2(CO)_8$ using a dual-stage temperature process at 175 and 160 °C, using PS-NH_2 (3) and PS-COOH (6) surfactants. Synthesis of 6 was conducted by the ATRP of styrene using functional initiator 5. Conditions: (a) styrene, CuBr, 2,2′-bipyridine, DMF, 110 °C; (b) thermolysis of the $Co_2(CO)_8$ at 175 °C, followed by growth at 160 °C for 30 min.

RESULTS AND DISCUSSION

The general approach that was developed to synthesize polymer-coated ferromagnetic NPs utilized a dual-stage temperature thermolysis of $Co_2(CO)_8$ in the presence of end-functional polystyrene surfactants (Scheme 1). End-functionalized polystyrenes bearing amine, phosphine oxide, or carboxylic acid ligands (PS-NH_2, PS-DOPO, and PS-COOH, respectively) were prepared using initiators **1**, **2** (Scheme 1), and **5** (Scheme 2) for ATRP. Using this process, well-defined polystyrenes with precise molar mass and composition were prepared. In the current report, we investigated the effect of different polymeric surfactant combinations on the decomposition of $Co_2(CO)_8$ for the preparation of ferromagnetic PS-CoNPs. These end-functional PS-NH_2, PS-DOPO, and PS-COOH are polymeric analogues to commonly used small-molecule surfactants of aliphatic/oleyl amines (AA), trioctylphosphine oxide (TOPO), and oleic acid (OA).[74,75] It has previously been shown that these small-molecule surfactants allowed for the preparation of a range of well-defined superparamagnetic and ferromagnetic CoNPs by combining these surfactants (*e.g.*, TOPO/OA, AA/TOPO) in different feed ratios. This previous work served as a reference point in our own synthesis using polymeric surfactants PS-NH_2 (**3**), PS-DOPO (**4**), (Scheme 1), and PS-COOH (**6**) (Scheme 2). Molar masses (number average, M_n) in the regime of M_n = 5000–10 000 g/mol were previously determined

to be optimal to afford ferromagnetic PS-CoNPs.[76] In the course of this investigation, we have developed a simplified synthesis of PS-CoNPs that was amenable to 820 mg quantities per batch of relatively uniformly sized ferromagnetic NPs with improved handling characteristics when isolated as powders.

Synthesis of End-Functionalized Polystyrene Surfactants. In the preparation of PS-NH_2 (**3**; M_n = 4800 g/mol; M_w/M_n = 1.08), initiator **1** was synthesized by the statistical coupling reaction of α,α′-dichloro-*p*-xylene (DCX) with potassium phthalimide and ATRP of styrene, followed by deprotection using hydrazine hydrate to afford **3** (Scheme 1). The synthesis of PS-DOPO (**4**; M_n = 4500 g/mol; M_w/M_n = 1.15) utilized the preparation of 4-(methoxymethyl)benzyl chloride, which was conducted *via* a statistical alkylation of DCX with $NaOCH_3$, followed by alkylation with dioctylphosphineoxide (DOPO) and deprotection with boron trichloride (BCl_3) to afford initiator **2**.[80–82] Initial attempts to directly alkylate DCX with stoichiometric amounts of DOPO resulted in unidentified byproducts that were most likely derived from the radical anionic species, as discussed by Rachon *et al.*[83] ATRP of styrene using initiator **2** yielded **4** (Scheme 1). Initiator **5** was commercially available and was directly used in the solution ATRP of styrene to afford PS-COOH (**6**; M_n = 9500 g/mol; M_w/M_n = 1.11; Scheme 2). All ATRP reactions used a copper(I) halide (chloride or bromide) and bipyridine (4,4′-dinonyl-2,2′-bipyridine or 2,2′-bipyridine) ligand-based catalyst system in the presence of *N*,*N*-dimethylformamide (DMF, 20% volume fraction) as a cosolvent to dissolve the copper complex. The use of DMF as a cosolvent afforded homogeneous conditions for ATRP and enabled direct use of initiators **2** and **5** without the need for protecting group strategies.[84]

Preparation of PS-CoNPs. Following the preparation of end-functionalized polystyrene surfactants **3**, **4**, and **6**, the synthesis of PS-CoNPs was investigated using a dual-stage temperature thermolysis of $Co_2(CO)_8$. Recently, Lin *et al.* demonstrated that uniformly sized superparamagnetic CoNPs (particle diameter (D) = 9.5 nm) could be prepared by using the small-molecule surfactants OA/TOPO along with a dual-stage temperature (180 and 130 °C) treatment.[85] In our modified dual-stage particle synthesis, a room-temperature solution of $Co_2(CO)_8$ was rapidly injected into a hot mixture of polymeric surfactants (T = 175 °C) to induce a rapid homogeneous nucleation of NPs and a subsequent drop in temperature to 160 °C. Growth of the CoNP was maintained at 160 °C for 30 min, yielding a viscous, stable ferrofluid. Initially, the dual-stage temperature treatment was evaluated using a mixture of PS-NH_2 (**3**) and PS-DOPO (**4**) prepared using ATRP as illustrated in Scheme 1. Transmission electron microscopy (TEM) images (Figure 1) of the resulting PS-CoNPs ($D_{PS\text{-}CoNPs}$ = 17 nm ± 1.8 nm) showed organization of dipolar colloids into extended nanoparticle chains when cast onto

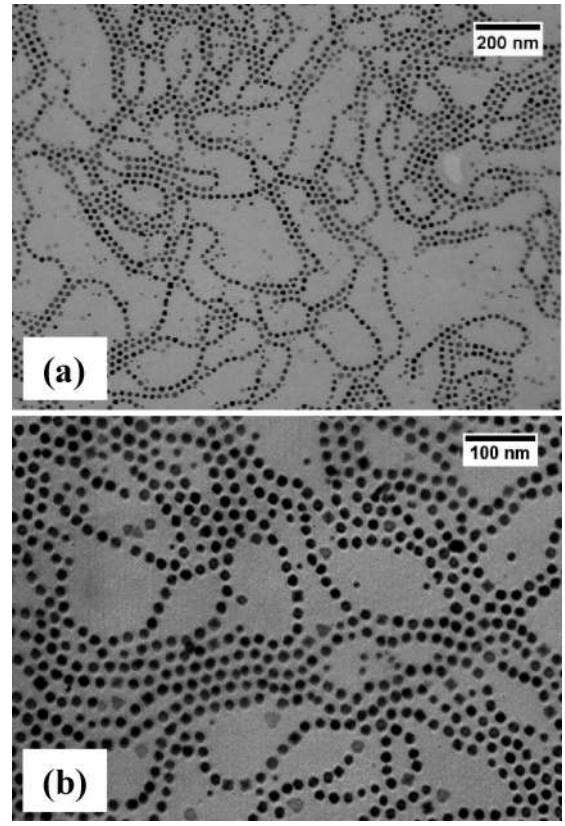

Figure 1. TEM micrographs of PS-CoNPs imaged at low (a) and high magnification (b), prepared using a mixture of PS-NH_2 (3) and PS-DOPO (4) in the thermolysis of $Co_2(CO)_8$ as shown in Scheme 1. The PS-CoNPs (as prepared; $D_{PS\text{-}CoNPs}$ = 17 nm ± 1.8 nm) were cast onto supported surfaces from a particle dispersion in toluene.

supporting surfaces from a toluene dispersion. An interesting additional phenomenon apparent in Figure 1 was the tendency of adjacent chains to form zippering configurations, where the chains were in close contact and the particles in the adjacent chain were centered in the gap regions between the particles. Recent simulations have indicated that this behavior was expected when strong mutual isotropic attractive (Yukawa) interactions were present, in addition to the directional dipolar interactions arising from the magnetic interactions.[86] We will return to a discussion of these interactions below.

Additionally, stable, redispersable powders could be recovered after precipitation due to the presence of a hairy polystyrene corona coordinated onto the CoNP surfaces. PS-CoNPs obtained from the current procedure possessed size and magnetic properties comparable to those of materials prepared using our previously reported methodology, where PS-NH_2 and PS-DOPO were synthesized using NMP.[76] This result confirmed that the size uniformity and magnetic properties of CoNPs synthesized from end-functional polystyrene surfactants were independent of the polymerization mechanism (*i.e.*, ATRP *versus* NMP) used to prepare the polymeric surfactants when using identi-

cal ligand chemistry and similar regimes of molar mass and polydispersity.

There is precedent for the feed ratios of metal precursor and surfactant to strongly affect particle size and magnetic properties.[68,72,74,87] Similar trends using PS-NH_2/PS-DOPO surfactants were observed, where a 4:1 mass ratio of $Co_2(CO)_8$ to polymeric surfactants was found to be optimal for the synthesis of ferromagnetic PS-CoNPs.[76] However, using the current synthetic conditions shown in Scheme 1, nearly uniform ferromagnetic PS-CoNPs were prepared ($D_{PS\text{-}CoNPs} \approx 17$ nm). This was found despite the variation in the feed of the metal precursors to the polymeric surfactants from 4:1 up to 1.5:1 mass ratios of $Co_2(CO)_8$ to PS-NH_2/PS-DOPO. PS-CoNPs prepared using this methodology contained a relative mass fraction of 40% of the organic polymer shell, in comparison to the 20% relative mass indicated in our previous report,[76] as determined by thermogravimetric analysis (TGA). While counter-intuitive, this series of experiments demonstrated that temperature conditions used in the thermolysis of $Co_2(CO)_8$ exhibited a stronger effect on particle size and magnetization than feed ratios of metal precursors to polymeric surfactants. Furthermore, the ability to add higher loadings of polymeric surfactant without compromising the growth of ferromagnetic CoNPs greatly improved the handling and storage characteristics of powders isolated by precipitation from stable ferrofluids. Isolated PS-CoNPs prepared from this process were easily dispersed in a wide range of nonpolar organic solvents (*e.g.*, toluene, chlorobenzene, tetrahydrofuran, dichloromethane) and were able to be stored in air without significant loss of magnetic properties over periods of weeks and months, as confirmed from vibrating sample magnetometry (VSM) and X-ray diffraction (XRD). However, one significant limitation of this dual-stage temperature process was that only ferromagnetic CoNPs could be prepared, as the synthesis of superparamagnetic CoNPs could not be accessed by variation of metal precursor/surfactant feed ratios. Further mechanistic studies on the growth mechanism of CoNP under these conditions are ongoing.

The strategy to prepare ferromagnetic PS-CoNPs was further expanded to other combinations of polymeric surfactants (PS-NH_2 (**3**) and PS-COOH (**6**)), as inspired by work using AA and OA small-molecule surfactant mixtures (Scheme 2).[74,75,88] This particular surfactant system was attractive, as carboxylic acid initiator **5** was commercially available and also able to be directly used in ATRP to prepare PS-COOH (**6**). The reaction conditions employed in the preparation of ferromagnetic PS-CoNP using **3** and **6** were identical to those used for PS-NH_2/PS-DOPO surfactants as previously discussed (Scheme 1). TEM images showed that relatively well-defined PS-CoNPs ($D_{PS\text{-}CoNPs} = 21$ nm $\pm$ 3.1 nm) were prepared using these conditions (Figure 2). While PS-CoNPs prepared using PS surfactants **3** and

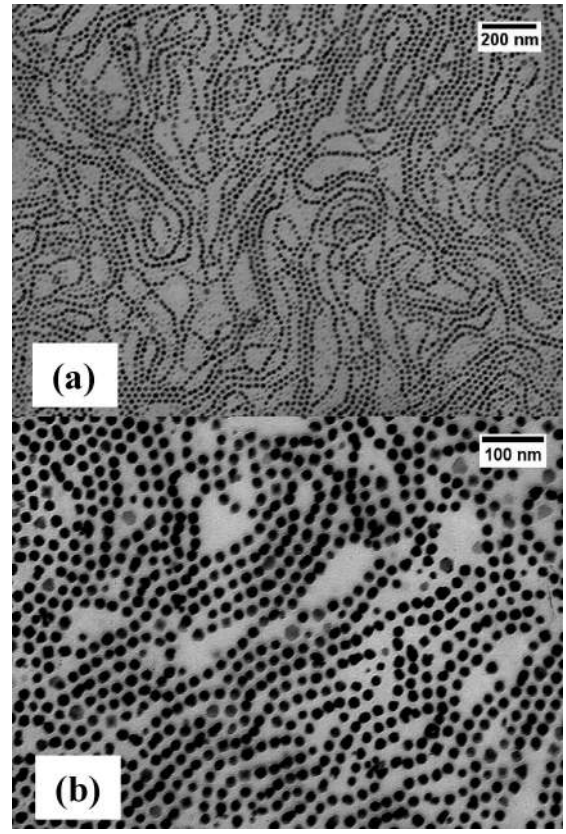

Figure 2. TEM images of self-assembled ferromagnetic PS-CoNPs ($D_{PS\text{-}CoNPs} = 21$ nm $\pm$ 3.1 nm) at low (a) and high magnification (b), prepared from a mixture of PS-NH_2 (3) and PS-COOH (6) in the thermolysis of $Co_2(CO)_8$. The PS-CoNPs were cast onto supporting surfaces from a particle dispersion in toluene.

6 were slightly larger than PS-CoNPs prepared from PS-NH_2/PS-DOPO surfactants, similar morphologies of nanoparticle chains were observed by TEM when the NPs were cast from toluene dispersions onto carbon-coated TEM grids.

Control experiments were performed using a single surfactant, either PS-NH_2 (**3**, Scheme 3) or PS-COOH (**6**, Scheme 4), in the dual-stage temperature thermolysis of $Co_2(CO)_8$. Surprisingly, when identical reactions were conducted using only **3** as a single surfactant system (Scheme 3), or surfactant combinations of **4** or **6**, similar particle sizes and morphologies were produced. TEM images (Figure 3) of the sample prepared from **3** showed relatively uniform particle size ferromagnetic

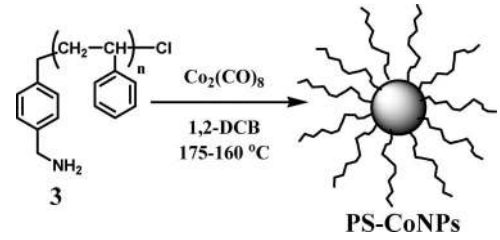

Scheme 3. Synthesis of PS-CoNPs using only PS-NH_2 (3) in the thermolysis of $Co_2(CO)_8$ at 175 and 160 °C. The thermolysis of $Co_2(CO)_8$ was performed at 175 °C, followed by growth at 160 °C for 30 min.

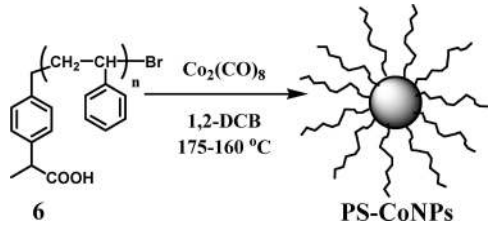

Scheme 4. Synthesis of PS-CoNPs using only PS-COOH (6) in the thermolysis of $Co_2(CO)_8$ at 175 and 160 °C. The thermolysis of $Co_2(CO)_8$ was performed at 175 °C, followed by growth at 160 °C for 30 min.

PS-CoNPs ($D_{PS\text{-}CoNPs}$ = 21 nm ± 2.9 nm) and the formation of self-assembled nanoparticle chains. However, additional control experiments using only **6** (Scheme 4) under the same conditions resulted in large-scale agglomeration and poorly defined PS-CoNPs of varying sizes and morphologies (Figure 4).

Using this simplified synthetic procedure, we then prepared larger quantities of ferromagnetic PS-CoNPs. While numerous reports have shown the ability to prepare both superparamagnetic and ferromagnetic NPs, the development of synthetic methods enabling access to larger quantities of ferromagnetic CoNPs that are able to be isolated and redispersed into organic media remains an important challenge. This synthetic method, using only PS-NH_2 (**3**), was particularly attractive for scaling up the preparation of ferromagnetic CoNPs, as ATRP could be used to prepare multigram quantities of **3** (see Experimental Section). By simply scaling up the quantities used in model small-scale particle reactions, isolated yields of 240, 400, and 820 mg of ferromagnetic PS-CoNPs were obtained. TEM confirmed that, for all conditions, particle sizes were in the range of 17–21 nm, with narrow size distributions (2–3 nm).

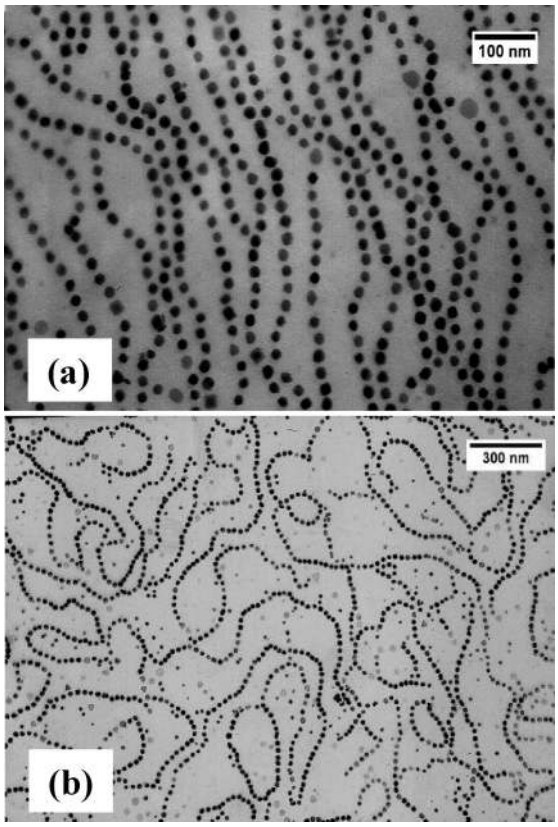

Figure 3. TEM images of PS-CoNPs at high (a) and low (b) magnification, prepared using only PS-NH_2 (3) in the thermolysis of $Co_2(CO)_8$. The PS-CoNPs (as prepared; $D_{PS\text{-}CoNPs}$ = 21 nm ± 2.9 nm) were cast onto supported surfaces from a particle dispersion in toluene.

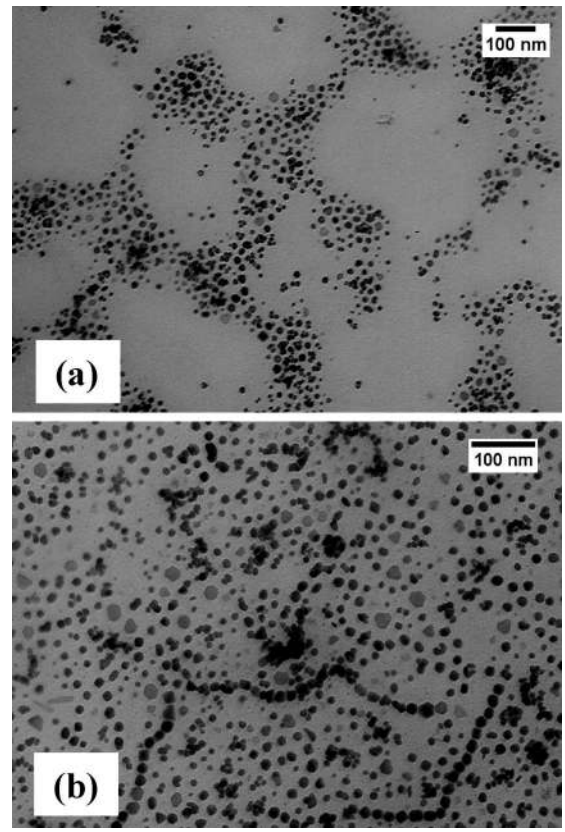

Figure 4. TEM images of self-assembled PS-CoNPs at low (a) and high magnification (b), prepared using the PS-COOH surfactant 6 as shown in Scheme 4. The PS-CoNPs (as prepared; $D_{PS\text{-}CoNPs}$ = 16 nm ± 4.5 nm) were cast onto supported surfaces from a particle dispersion in toluene.

Characterization of PS-CoNPs. XRD was used to investigate the effect of different polymeric surfactants on the crystalline phases of metallic CoNPs prepared using the dual-stage temperature thermolysis reaction at 175 and 160 °C. For all experiments conducted using mixtures of polystyrene surfactants, or only PS-NH_2 (**3**) as discussed in Schemes 1–3, the formation of primarily the epsilon (ϵ) Co crystalline phase was observed.[89,90] This result was contrary to our previous report using PS-NH_2 and PS-DOPO surfactants prepared from NMP in the thermolysis of $Co_2(CO)_8$ at 180 °C. The formation of ϵ-Co was likely a metastable condition that was favored as a consequence of using the 175 and 160 °C dual-stage thermolysis procedure to prepare ferromagnetic PS-CoNPs. XRD measurements on the PS-CoNPs prepared using PS-COOH (**6**) alone suggested that the majority of these particles adopt the ϵ-Co crystal phase. However, the XRD pattern appeared as a broad peak,

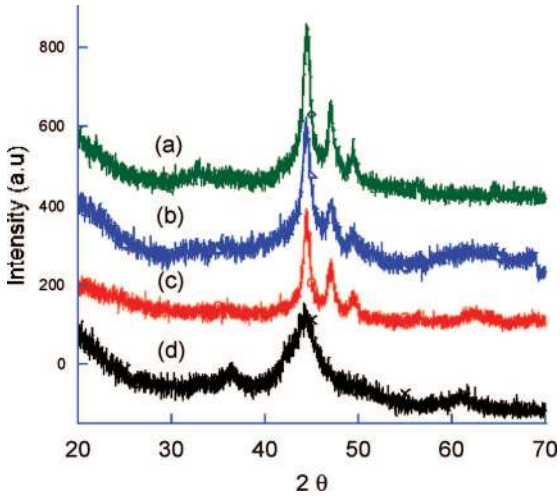

Figure 5. XRD patterns of PS-CoNPs prepared from (a) PS-NH_2 (3), (b) a mixture of surfactants PS-NH_2 (3) and PS-COOH (6), (c) a mixture of PS-NH_2 (3) and PS-DOPO (4), and (d) PS-COOH (6), where all polymeric surfactants were synthesized using ATRP.

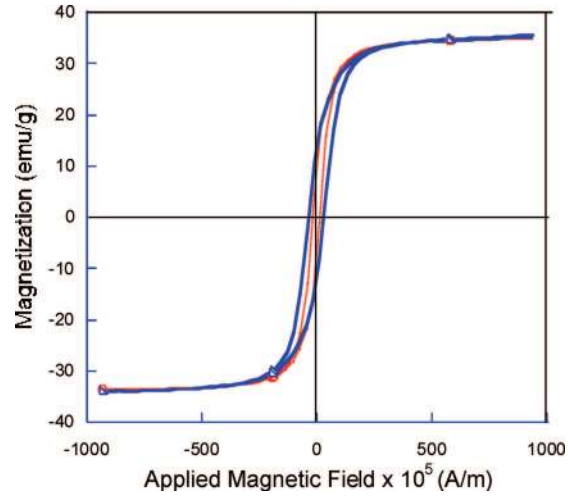

Figure 6. Magnetization *versus* applied magnetic field for ϵ-cobalt nanoparticles prepared from PS-NH_2 (3) with an average diameter of 21 nm. The thin red trace shows VSM measurement at room temperature, while the thick blue trace corresponds to $T = -266$ °C (77 K).

which indicated that the sample was amorphous and ill-defined. To determine if the polymerization mechanism used to prepare polymeric surfactants (*i.e.*, ATRP *versus* NMP) affected the crystalline phase of CoNPs, an additional control experiment was conducted using PS-NH_2 and PS-DOPO surfactants prepared from NMP using a 175 and 160 °C dual-stage temperature process. ϵ-Co NPs ($D_{PS\text{-}CoNPS} = 16$ nm $\pm$ 2.4 nm) were also prepared with these polymeric surfactants, confirming that the method of polymerization used to prepare end-functional polystyrenes (*i.e.*, ATRP *versus* NMP) did not affect the size or the crystalline phase of PS-CoNPs formed under these conditions.

Magnetic properties of the PS-CoNPs prepared from different surfactants systems, as illustrated in Schemes 1–4, were measured using VSM at room temperature and −266 °C (77 K). Magnetic measurements confirmed that all of the prepared hybrid nanocomposites were weakly ferromagnetic at room temperature and strongly ferromagnetic at −266 °C. PS-CoNPs that were prepared using surfactants PS-NH_2 (**3**) and PS-DOPO (**4**) were comparable in particle size ($D = 17$ nm), saturation magnetization ($M_s = 44$ emu/g), and magnetic coercivity ($H_c = 10500$ A/m) to materials prepared using our previously reported methodology.[76] However, a small increase in the coercivity of PS-CoNPs was observed when polymeric surfactants **3** and PS-COOH (**6**) were employed in the particle synthesis ($M_s = 35.1$ emu/g; $H_c = 16100$ A/m), presumably due to the slightly larger particle size ($D = 21$ nm).

VSM of PS-CoNPs prepared using only **3** is shown in Figure 6 ($M_s = 34.2$ emu/g; $H_c = 20700$ A/m). The magnetic behavior of PS-CoNPs prepared using only **3** (as shown in Scheme 3), as judged from plots of magnetization (*M*) *versus* applied field strength (*H*), closely resembled that of PS-CoNPs prepared using a mixture of PS surfactants (Schemes 1 and 2) at both room temperature and −266 °C. PS-CoNPs prepared using only **6** consisted of a mixture of ferromagnetic, antiferromagnetic, and diamagnetic materials, as suggested by the large increase of magnetic coercivity ($H_c = 101000$ A/m) at −266 °C. The presence of antiferromagnetic materials required higher magnetic fields to reorient spins in the opposite direction. The magnetic properties of PS-CoNPs prepared from **6**, measured at low temperature, were consistent with the poorly defined particle size (Figure 4) and low degree of crystallinity observed from XRD (Figure 5d).

Morphologies of Dipolar Assemblies of PS-CoNPs. Numerous computational studies have indicated that a diversity of possible self-assembled structures should form in suspensions of dipolar NPs, depending on an interplay among the particle concentration, the strength of the dipolar interaction, and the strength of the isotropic attractive interparticle interaction responsible for phase separation.[11,13,14,39,86,91–95] The formation of anisotropic chain-like mesostructures has long been known to arise in particle systems where interactions were dominated by strong long-range dipole–dipole interactions that must exceed contributions from thermal fluctuations. In this report, we observe the self-assembly of PS-CoNP chains, which was characteristic of this type of assembly when the nanoparticle dispersion was cast from solution onto supporting surfaces to form a variety of discrete dipolar assemblies. The PS-CoNPs used in these studies all possessed comparable particle size ($D = 21$–22 nm) and magnetic properties ($M_s = 30$–40 emu/g; $H_c = 16000$–24000 A/m). These preliminary studies also provide evidence of the subtle interactions between these chain structures that have been observed previously only in simulation studies. For example, the relatively high concentrations of our nano-

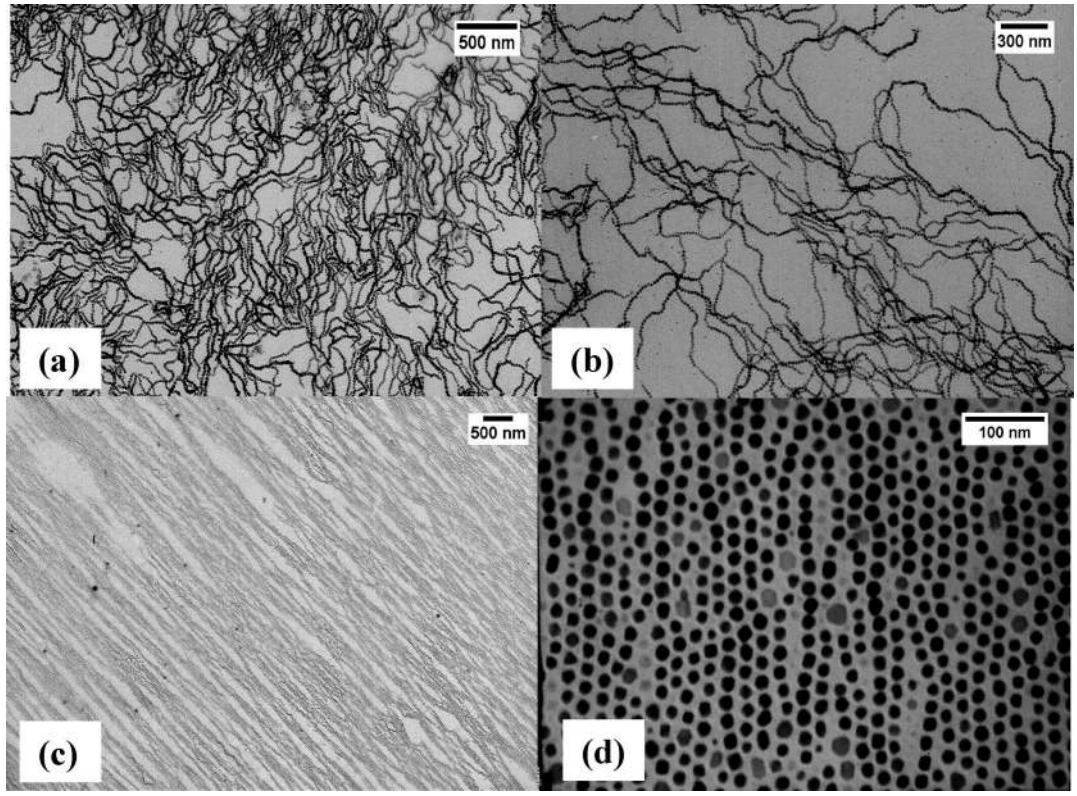

Figure 7. (a,b) TEM images of randomly entangled chains of PS-CoNP (D = 21 nm ± 3 nm) cast from a toluene dispersion (c = 0.5 mg/mL) in zero-field. (c) TEM image of aligned chains of PS-CoNPs (D = 21 nm ± 2.9 nm) cast from a dichlorobenzene dispersion (c = 0.5 mg/mL) in 100 mT. (d) High magnification TEM image of aligned PS-CoNP chains from (c).

particle dispersions allowed us to observe local nematic interactions that evidently caused the formation of appreciable domains where the dipolar chains shared a common orientation. It is our impression that these chain interactions make the chain structure more persistent (*i.e.*, enhance chain stiffness), an effect that requires further quantification. We also see the formation of "zippered" chain configurations (see Figure 1 for a particularly good example), where the chains form side-by-side configurations even at low particle concentrations. The simulations reported by Weis[86] show that such structures were energetically favored when appreciable isotropic attractive interactions were present (arising mainly from the grafting chains in the present experimental study) in addition to strong dipolar interactions. Our previous work on these PS-CoNP chains segregated to oil–water interfaces have indicated that the attractive interparticle interactions can be strong enough to induce chains to collapse into ball-like configurations on long time scales.[38] All of these general patterns of behavior have been predicted from Monte Carlo simulations[86,96–98] of the self-assembly of dipolar particles with additional isotropic attractive interactions. Future work to establish the interactions involved in these particle systems is underway to allow a more quantitative comparison with these simulations. From these previous simulation studies, we infer that there are numerous experimental handles that can be used to control the morphology, and we have indeed verified that the nanoparticle morphologies are highly dependent on nanoparticle concentration, the magnetic properties of the particles themselves, the external magnetic field strength, and the choice of solvent when the nanoparticle solutions are cast onto carbon-coated copper TEM grids.

Dipolar assembly of self-assembled correlated domain structures (Figure 7a), randomly entangled chains (Figure 7b), or nematic-like field-aligned mesostructures (Figure 7c,d) can be easily obtained using a variety of organic solvents as the dispersing media and an external field. These types of assemblies have been observed in numerous reports of both simulations and imaging experiments. The formation of micrometer-sized 1-D mesostructures using ferromagnetic PS-CoNPs (D = 21 nm; PS shell corresponds to M_n = 4800 g/mol) was confirmed when organic colloidal dispersions were cast onto carbon-coated TEM grids. The formation of these types of morphologies, when cast from dilute particle dispersions, indicated that dipolar interactions dominated the assembly process in the organization of dipolar NPs into mesoscopic chains.[11,14,95]

The formation of flux-closure rings or "bracelet" dipolar assemblies has been reported from experiments in which ferromagnetic CoNPs were prepared using small-molecule surfactants.[17–19,74] While the formation of looped bracelets was entropically unfavorable, the assembly of dipoles into a closed circuit minimized both the magnetic moment and the field outside of the ring-

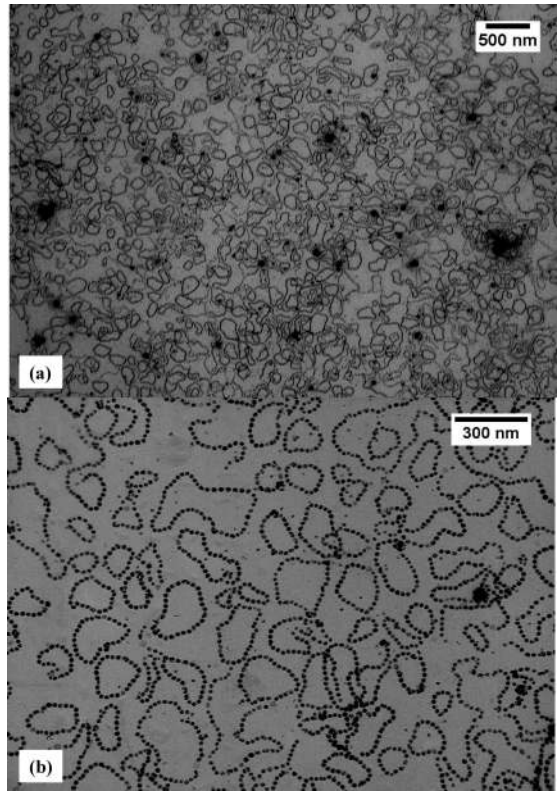

Figure 8. (a) TEM image of bracelet flux-closure rings of PS-CoNPs (D =21 nm ± 3.3 nm) cast from a chlorobenzene dispersion (c = 0.5 mg/mL) in zero-field. (b) High magnification TEM image of the PS-CoNP assemblies from (a) which are consistent with Monte Carlo simulations reported by Douglas *et al.*[97]

like structure. The formation of bracelet-like assemblies was observed using PS-CoNPs when colloidal dispersions were drop-cast from a less volatile organic solvent (chlorobenzene) and a slightly higher molecular weight (MW) PS surfactant (M_n = 12000 g/mol; M_w/M_n = 1.10) for the preparation of PS-CoNPs. Particle concentrations of 0.5 mg/mL were found to be optimal to afford bracelet assemblies, as higher and lower concentrations tended to afford linear chains. It is important to note that, while the formation of bracelets was the preferred morphology for these PS-CoNPs, numerous defects structures were also typically observed in the form of short linear chains or branched assemblies, an effect also established in simulations of strongly interacting dipolar fluids.[96] TEM images of the dipolar assemblies formed from PS-CoNPs with lower MW PS surfactants, shown in Figure 7 (M_n = 4800 g/mol for each system in Figure 7), exhibit dramatically different morphologies than for bracelet-type structures formed from PS-CoNPs prepared using higher MW PS surfactants cast from chlorobenzene (Figure 8). These images confirm that the ferromagnetic NPs form rings of varying size in the range of 10–100 colloids per colloidal assembly. The use of a less volatile solvent, such as chlorobenzene, led to a higher yield of these ring structures when the dispersion was cast onto carbon-coated copper TEM grids in the absence of an applied magnetic field. Deposition of PS-CoNPs from more volatile solvents, such as tetrahydrofuran or dichloromethane, resulted in the formation of predominately short linear chains. This observed solvent dependence on ring formation is contrary to a recent report, in which poly(vinylpyrrolidone)-coated magnetite nanoparticles were used.[19] The cause of these differences is currently under investigation and is complicated by the inherent differences in the nature of these materials. The presence of a higher MW PS-NH_2 surfactant (M_n = 12 000 g/mol) was also critical to ring self-assembly. The assembly of PS-CoNPs with a lower MW PS surfactant (M_n = 4800 g/mol) cast from chlorobenzene under identical conditions did not lead to rings, as will be discussed in later sections. Since the stiffness of the nanoparticle chains evidently increases with the strength of the dipolar interaction and the formation of dipolar chains of significant length increases with increasing chain stiffness, we can understand this trend with polymeric surfactant MW to arise from an increased separation of the dipolar particles and a corresponding weakening of the dipolar interactions with higher molar masses. Correspondingly, recent rule-based simulations of dipolar particle assembly have provided evidence for an enhanced tendency toward ring assembly upon lowering the strength of the dipolar particle interaction.[39]

A conspicuous aspect of the self-assembled rings in Figure 8 is that the rings are neither knotted nor catenated. Unknotted rings or zippered rings are the lowest energy structure for dipolar particles with a strong dipolar interaction,[99] but recent calculations also indicate that, if there are both directional dipolar and isotropic van der Waals interactions that are comparable in magnitude, then the low-energy ring configurations involving nontrivial knot complexity may arise from the competing tendencies of the dipolar interaction to establish an open ring structure and the van der Waals interaction to drive the particle clusters into spherical droplet configurations.[100] Since we can tune the strength of the van der Waals interaction by varying the polymer surfactant molecular mass, we should be able to search for these knotted structures in the future.

As was alluded to previously, the formation of a nematic-like ordering of ferromagnetic PS-CoNPs was observed only when colloids were prepared using lower MW PS surfactant (M_n = 4800) and then cast from a chlorobenzene dispersion (Figure 9). Unlike the previously discussed bracelet morphology, under identical conditions and zero-field, the organization of nanoparticle chains exhibited local ordering of colloids into a "lamellae"-like folding of 1-D assemblies. This particular type of organization was observed for PS-CoNPs cast from nonpolar and relatively nonvolatile solvents, such as chlorobenzene and toluene, while more volatile solvents (THF, CH_2Cl_2) led to linear nanoparticle chains

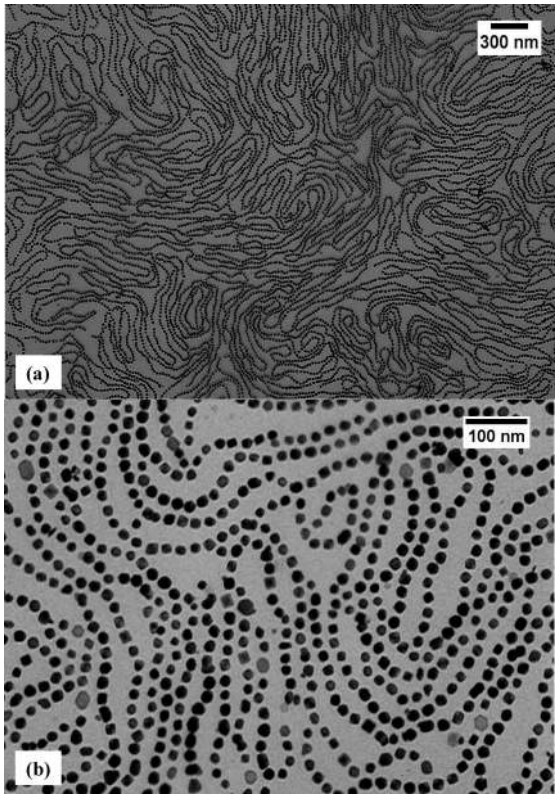

Figure 9. (a) TEM image of self-assembled PS-CoNPs (D = 21 nm ± 2.9 nm) exhibiting local nematic LC ordering cast from a chlorobenzene particle dispersion (c = 0.5 mg/mL) in zero-field. (b) High magnification TEM image of PS-CoNP assemblies from (a). These simulations resemble morphologies found in the Monte Carlo simulations reported by Weis *et al.*[86]

having an appearance similar to random walk chains. The formation of the folded lamellae nanoparticle chains was found to be prevalent in dilute particle concentration regimes (0.5 mg/mL). Similar morphologies were found previously in the Monte Carlo simulations reported by Weis *et al.*, where dense arrays of self-ordered 1-D mesostructures arose from both dipolar interactions forming chains, in conjunction with lateral associations of nanoparticle chains *via* anti-parallel configurations of the magnetic moments.[86] Although these structures are "expected", these dipolar nematic LC self-assembly patterns have not been observed experimentally in ferromagnetic nanoparticle dispersions. While the mechanism of this type of local nematic ordering is still under investigation, it is anticipated that the presence of macromolecular PS surfactants enhanced short-range van der Waals associations, which facilitated lateral nanoparticle association of anti-parallel dipole moments.

CONCLUSION

The preparation and characterization of ferromagnetic polystyrene-coated cobalt nanoparticles is reported. The use of these synthetic routes using ATRP enabled the synthesis of multigram quantities of end-functional polystyrenic surfactants. The preparation of polymer-coated ferromagnetic colloids was also improved by the utilization of a dual-stage temperature thermolysis protocol that enabled the synthesis of polystyrene-coated ferromagnetic nanoparticles of cobalt on a nearly 1-g scale per reaction. Using these well-defined ferromagnetic nanoparticles, a novel magnetically assembled morphology was observed when the nanoparticles were cast onto supporting surfaces. The mesostructures formed from self-assembly of dipolar nanoparticles drop-cast from solution onto substrates were found to be consistent with recent theoretical modeling, and we look forward to fundamental studies of self-assembly based on these model particles.

EXPERIMENTAL SECTION

Materials and Characterization. Anhydrous 1,2-dichlorobenzene (DCB), toluene, neutral alumina, 1,4,7,10,13,16-hexaoxacyclooctadecane (18-crown-6), acetonitrile (ACN), acetone, dichloromethane (DCM), hexanes (HEX), methanol (MeOH), *N*,*N*- dimethylformamide (DMF), hydrazine hydrate, magnesium sulfate, copper(I) chloride, 2,2′-bipyridyl (bipy), 4,4′-dinonyl-2,2′-bipyridyl (dNbipy), boron trichloride (1 M solution in DCM), sodium hydride (96%), α,α′-dichloro-*p*-xylene (DCX), and 2-[4-(bromomethyl)phenyl]propionic acid were purchased from Aldrich and used as received without further purification. Copper(I) bromide was purified by stirring in glacial acetic acid overnight. Styrene was purchased from Aldrich and passed through a short column of neutral alumina to remove inhibitors prior to use in polymerizations. Deoxygenation of monomers, solvents, and reaction mixtures was achieved by bubbling with argon gas for 30 min prior to use in polymerizations.

Dicobaltoctacarbonyl ($Co_2(CO)_8$) was purchased from Strem Chemicals and used as received. Thermolysis reactions were performed using an Omega temperature controller with a home-made K-type thermocouple and the PowerStat variable autotransformer at level 70/140. Flash chromatography was performed using silica gel from VWR (230–400 mesh) and TLC plates coated with silica gel 60 F254 (Merck). Nuclear magnetic resonance (NMR) spectroscopy was performed using Bruker DRX 500 MHz FT-NMR and Bruker DRX 250 MHz FT-NMR spectrometers, operating with XWinNMR software (Bruker). Size exclusion chromatography (SEC) was performed in a tetrahydrofuran (THF) mobile phase with a Waters 1515 isocratic pump running three 5-μm PLgel columns (Polymer Labs, pore sizes 10^4, 10^3, and 10^2 Å) at a flow rate of 1 mL/min with a Waters 2414 differential refractometer and a Waters 2487 dual-wavelength UV–vis spectrometer. Molar masses were calculated using the Empower software (Waters), calibrating against low-polydispersity linear polystyrene standards. TEM images were obtained on a JEM100CX II transition electron microscope (JEOL) at an operating voltage of 60 kV, using in-house-prepared copper grids (Cu, hexagonal, 300 mesh). Analysis of images was carried out using ImageJ software (W. S. Rasband, National Institutes of Health, 1997–2007, http://rsb.info.nih.gov/ij/). Relative uncertainty of particle size determinations using ImageJ was found to be 1% of the diameter average (*e.g.*, 20 nm ± 0.2 nm). VSM measurements were obtained using a Waker HF 9H electromagnet with a Lakeshore 7300 controller and a Lakeshore 668 power supply. Magnetic measurements were carried out at room temperature (27 °C, 300 K) and low temperature (−266 °C or 77 K), with a maximum S-2 applied field of 1190 kA/m, a ramp rate of 2630 A m^{-1} s^{-1}, and a time constant of 0.1. XRD measurements were performed using the X'pert X-ray diffractometer

(PW1827, Phillips) at room temperature with a CuKα radiation source at 40 kV and 30 mA.

Note. Identification of commercial products is made only to facilitate reproducibility and to adequately describe the procedure. In no case does it imply endorsement by NIST or that the named product is necessarily the best product for the procedure.

Preparation of 4-(Chloromethyl)benzyl Phthalimide (1). To an oven-dried three-neck round-bottom flask were added α,α′-dichloroxylene (6.59 g, 3.76×10^{-2} mol), potassium phthalimide (2.67 g, 1.44×10^{-2} mol), and 18-crown-6 (0.240 g, 9.08×10^{-4} mol), and the solids were then dissolved in ACN (75 mL). The reaction mixture was refluxed overnight under argon, filtered through a coarse glass frit, washed with acetone, and concentrated *in vacuo* to yield a white solid. The crude product was purified *via* flash chromatography eluting with a 1:1 HEX/DCM mixture with a gradual increase to DCM to yield a white crystalline solid (2.70 g, 67%, R_f = 0.2, 2:1 DCM/HEX). ^{1}H NMR (500 MHz, $CDCl_3$, δ): 7.85 (dd, J = 5 Hz, 3 Hz, Ar H, 2H), 7.71 (dd, J = 5.5 Hz, 3 Hz, Ar H, 2H), 7.45–7.34 (m, Ar H, 4H), 5.3 (s, CH_2, 2H), 4.55 (s, CH_2, 2H). ^{13}C NMR (125 MHz, $CDCl_3$, δ): 167.79, 136.97, 136.49, 133.92, 131.94, 128.90, 128.81, 123.24, 45.73, 41.13. HRMS: exact mass calculated for $[M + 1]^+$ $C_{16}H_{12}O_2ClN$, 287.0518; found, 285.0527.

Preparation of Benzyl Phthalimide End-Functionalized Polystyrene (1b). To a 25 mL Schlenk flask equipped with a stir bar were added **1** (0.500 g, 1.75×10^{-3} mol), Cu(I)Cl (0.173 g, 1.75×10^{-3} mol), and bipy (0.546 g, 3.50×10^{-3} mol). The flask was fitted with a rubber septum, evacuated, and back-filled with argon for three cycles, and the flask contents were left under argon. Deoxygenated DMF (2 mL) was added to the flask *via* syringe and stirred at room temperature until a red complex formed. Deoxygenated styrene (10.9 g, 12.0 mL, 1.05×10^{-1} mol) was added directly into the flask. The flask was placed in a thermostated oil bath held at 110 °C for 16 h to reach a monomer conversion of 80%. The reaction mixture was diluted in 300 mL of DCM and passed through an alumina plug to remove the copper catalyst. The polymer solution was concentrated and precipitated into stirring methanol (1000 mL) twice, followed by drying *in vacuo* to yield a white powder (7.71 g, 89% yield based on monomer conversion). ^{1}H NMR (250 MHz, $CDCl_3$, δ): 7.82 (b, Ar H, 2H), 7.67 (b, Ar H, 2H), 7.10–6.50 (bm, Ar H), 4.77 (bm, CH_2), 2.4–1.2 (bm, CH + CH_2). $M_{n\ SEC}$ = 4800 g/mol; M_w/M_n = 1.08.

Reduction of Phthalimide Functionality with Hydrazine Hydrate (PS-NH_2, 3). To a round-bottom flask equipped with a stir bar was added **1b** (7.71 g, 1.61×10^{-3} mol), which was then dissolved in THF (50 mL). Methanol (5 mL) was added dropwise, followed by the addition of hydrazine hydrate (0.640 g, 1.28×10^{-2} mol). The flask was fitted with a rubber septum, and the reaction mixture was stirred at room temperature for 24 h, after which a white precipitate was observed. The reaction mixture was concentrated and redissolved in THF, followed by precipitation into stirring methanol (1000 mL). The precipitation was repeated twice, followed by drying *in vacuo* to yield the amine end-functionalized polystyrene as a white powder (7.20 g, 93%). ^{1}H NMR (250 MHz, $CDCl_3$, δ): 7.10–6.50 (bm, Ar H), 3.85–3.75 (bm, CH_2), 2.40–1.20 (bm, CH + CH_2).

Preparation of Carboxylic Acid End-Functionalized Polystyrene (PS-COOH, 6). To an oven-dried 125 mL Schenk flask equipped with a stir bar were added Cu(I)Br (0.361 g, 2.52×10^{-3} mol), 2-[4-(bromomethyl)phenyl]propionic acid (**5**, 0.650 g, 2.50×10^{-3} mol), and bipy (0.786 g, 5.04×10^{-3} mol). The flask was fitted with a rubber septum, evacuated, and back-filled with argon for three cycles. Deoxygenated DMF (7 mL) was added *via* syringe and stirred until a red complex formed. Deoxygenated styrene (34.5 g, 38.0 mL, 3.28×10^{-1} mol) was added *via* syringe to the reaction flask. The flask was placed in a thermostated oil bath held at 110 °C for 16.5 h to reach a monomer conversion of 63%. The reaction mixture was diluted in 300 mL of DCM and passed through a short alumina column to remove the copper catalyst. The polymer solution was concentrated and precipitated into stirring methanol twice, followed by drying *in vacuo* to yield a white powder (17.9 g, 82% yield based on monomer conversion). ^{1}H NMR (250 MHz, $CDCl_3$, δ): 7.10–6.50 (bm, Ar H), 2.40–1.20 (bm, CH + CH_2). $M_{n\ SEC}$ = 9500 g/mol; M_w/M_n = 1.11.

Preparation of 1-(Chloromethyl)-4-(methoxymethyl)benzene (2a). To an oven-dried three-neck round-bottom flask was added α,α′-dichloroxylene (14.0 g, 8.00×10^{-2} mol), and solids were dissolved in THF (90 mL) under argon. Sodium methoxide (3.00 g, 5.55×10^{-2} mol) was dissolved in methanol (50 mL) and slowly added *via* syringe. The reaction was stirred under argon overnight at room temperature. The reaction mixture was filtered and quenched with HCl (0.1 M in deionized (DI) water, 4 mL). The filtrate was extracted with DI water twice and once with saturated brine. The combined organic layer was dried over magnesium sulfate and filtered, and the solution was concentrated under reduced pressure to yield a yellow oil. The yellow oil was purified *via* flash chromatography with an initial 6:1 HEX/DCM elution mixture with a gradual increase to 1:1 HEX/DCM to yield a yellow oil (4.60 g, 67% reaction yield). ^{1}H NMR (500 MHz, $CDCl_3$, δ): 7.38–7.31 (m, Ar H, 4H), 4.57 (s, CH_2Cl, 2H), 4.46 (s, CH_2O, 2H), 3.39 (s, OCH_3, 3H). ^{13}C NMR (125 MHz, $CDCl_3$, δ): (138.34, 136.50, 128.61, 128.33, 127.59, 57.84, 45.74). MS (EI^+): m/z 171.04 $[M + H]^+$.

Preparation of 4-(Methoxymethyl)benzyl Dioctylphosphine Oxide (2b). To an oven-dried 100 mL three-neck round-bottom flask equipped with a magnetic stir bar and condenser was added dioctylphosphine oxide (1.30 g, 4.75×10^{-3} mol).[81,82] Anhydrous THF (30 mL) was added to dissolve the solids, followed by addition of NaH (0.200 g, 8.33×10^{-3} mol). The white suspension was heated at reflux temperature for 30 min under argon. A solution of **2a** (0.540 g, 3.17×10^{-3} mol) in 3 mL of anhydrous THF was added dropwise *via* syringe. The reaction mixture was heated at reflux overnight under argon. Solvent was removed under reduced pressure to yield a yellow oil. The yellow oil was dissolved in DCM and purified *via* flash chromatography (1:0.3 DCM/diethyl ether mixture followed by 1:0.1 DCM/MeOH) to yield a white crystalline solid (0.780 g, 52%). ^{1}H NMR (500 MHz, $CDCl_3$, δ): 7.39–7.22 (b, Ar H, 4H), 4.44 (s, CH_2Ph, 2H), 3.39 (s, CH_3O, 3H), 3.12 (d, J = 14 Hz, CH_2PO, 2H), 1.58 (m, CH_2, 8 H), δ 1.26 (m, CH_2, 20H), 0.88 (t, CH_3, 6H). ^{13}C NMR (125 MHz, CDCl3, δ): 136.77, 131.85, 129.43, 128.13, 74.30, 58.15, 36.04 (d, J = 59 Hz, CH_2PO), 31.77, 31.16, 31.05, 29.08, 27.36 (d, J = 32.63 Hz, CH_2PO), 22.61, 21.61, 14.08. HRMS: exact mass calculated for $[M + 1]^+$ $C_{25}H_{45}O_2P$, 409.3235; found, 409.3247.

Preparation of 4-(Chloromethyl)benzyl DOPO (Initiator 2). Chloromethylation of 4-(methoxymethyl)benzyl dioctylphosphine oxide was performed according to a modification of a procedure reported elsewhere.[101,102] To an oven-dried three-neck round-bottom flask was added 4-(methoxymethyl)benzyl dioctylphosphine oxide (0.780 g, 1.91×10^{-3} mol), and the solids were then dissolved in DCM (8 mL). The solution mixture was cooled to 0 °C using an ice bath. Boron trichloride solution (4.00 mL, 4.00×10^{-3} mol) was added dropwise into the reaction mixture using a syringe. The mixture was stirred at 0 °C for 2 h under argon. The reaction mixture was quenched with methanol, and then the mixture was poured into a stirred solution of 5% NaOH (50 mL), cooled in ice. The layers were separated, and the aqueous layer was then twice extracted with DCM. The combined organic layer was washed with DI water, dried over magnesium sulfate, and filtered, and the solvent was concentrated under reduced pressure to afford a yellow oil. The oil was purified *via* flash chromatography (1:0.2 DCM/diethyl ether) to yield the product as a white crystalline solid (0.780 g, 52% reaction yield). ^{1}H NMR (250 MHz, $CDCl_3$, δ): 7.33 (dd, J = 28 Hz, 8 Hz, 4H), 4.58 s, CH_2Cl, 2H), 3.12 (d, J = 14 Hz, CH_2PO, 2H), 1.58 (m, CH_2, 8H), 1.26 (m, CH_2, 20H), 0.88 (t, CH_3, 6H). ^{13}C NMR (125 MHz, $CDCl_3$, δ): 136.07, 132.81, 129.81, 129.01, 45.86, 36.08 (d, J = 58 Hz, CH_2PO), 31.78, 31.17, 31.06, 29.08, 27.55 (d, J = 65 Hz, CH_2PO), 22.62, 21.67, 14.08. HRMS: exact mass calculated for $[M + 1]^+$ $C_{24}H_{43}ClOP$, 413.2740; found, 413.2723.

Preparation of Benzyl DOPO End-Functionalized Polystyrene (PS-DOPO, 4). To a 10 mL Schlenk flask were added **2** (0.300 g, 7.28×10^{-4} mol), Cu(I)Cl (0.072 g, 7.27×10^{-4} mol), and dNbipy (0.600 g, 1.46×10^{-3} mol). The flask was fitted with a rubber septum, evacuated, and back-filled with argon three times, and the solution was left under argon. Deoxygenated styrene (4.50 g, 5.00 mL, 4.33×10^{-2} mol) was added *via* syringe to the flask and allowed to stir at room temperature until the catalyst was dissolved. The flask was placed into a thermostated oil bath held

at 110 °C for 4 h to reach a monomer conversion of 60%. After the heating was stopped, the reaction mixture was diluted in 200 mL of DCM and passed through a short alumina column. The polymer solution was concentrated and precipitated into methanol twice, followed by drying *in vacuo* to yield DOPO end-functionalized polystyrene as a white powder (1.70 g, 63% yield based on monomer conversion). ^{1}H NMR (500 MHz, $CDCl_3$, δ): 7.15–6.43 (bm, ArH), 4.6–4.3 (bm, 1H, CHCl), 3.11–3.06 (bm, 2H, CH_2PO), 2.27–1.30 (bm, CH + CH_2), 0.94–0.88 (b, CH_3). $M_{n\ SEC}$ = 4500 g/mol; M_w/M_n = 1.15.

Preparation of PS-CoNPs Using End-Functionalized Polystyrene Surfactants, PS-NH_2 (3) and PS-DOPO (4). To an oven-dried 100 mL three-neck round-bottom flask equipped with a stir bar and condenser were added PS-NH_2 (**3**, 0.160 g, 3.33×10^{-2} mmol) and PS-DOPO (**4**, 0.040 g, 8.89×10^{-3} mmol). Polymers **3** and **4** were dissolved in anhydrous DCB (20 mL) and heated to reflux under argon. A solution of $Co_2(CO)_8$ (0.300 g, 8.77×10^{-4} mol) dissolved in anhydrous DCB (4 mL) was rapidly injected into the hot mixture (175 °C). Upon injection, the reaction temperature dropped to 160 °C, and the reaction mixture was maintained at 160 °C for 30 min. The reaction mixture was then cooled to room temperature under argon. The as-prepared ferrofluid (0.5 mL) was diluted in chlorobenzene (10 mL) for TEM imaging and analysis. A drop of this nanoparticle solution was cast onto a carbon-coated copper grid and allowed to dry at room temperature. To isolate the polystyrene-coated cobalt nanoparticle, the ferrofluids were precipitated into stirring hexanes (500 mL) to yield a black precipitate that was collected by sedimentation using a standard AlNiCo magnet and decanting of the hexanes phase. The resulting precipitate was dried *in vacuo* to yield a black powder (yield = 120 mg) that was soluble in a variety of organic solvents (*e.g.*, toluene, THF, DCM) and was responsive to an external magnetic field. TGA revealed that an organic content of 43% relative mass to the polymeric surfactant shell was present in the isolated product. The particle size of the PS-CoNPs (D =17 nm ± 1.8 nm) was determined by TEM. Magnetic properties of PS-CoNPs were measured using VSM at room temperature: M_s = 44 emu/g; H_c = 10500 A/m (131 Oe).

Preparation of PS-CoNPs Using End-Functionalized Polystyrene Surfactants, PS-NH_2 (3) and PS-COOH (6). To an oven-dried 100 mL three-neck round-bottom flask equipped with a stir bar and condenser were added PS-NH_2 (**3**, 0.160 g, 3.33×10^{-2} mmol) and PS-COOH (**6**, 0.040 g, 4.21×10^{-3} mmol). The polymers were dissolved in DCB (20 mL), and the solution was heated to 175 °C. Separately, $Co_2(CO)_8$ (0.300 g, 8.77×10^{-4} mol) was dissolved in DCB (4 mL) at room temperature in air and was rapidly injected into the hot polymer solution. The heating protocols followed were identical to those discussed previously. PS-CoNPs were purified by precipitation into hexanes (500 mL), yielding a black powder (yield = 240 mg). The particle size of the PS-CoNPs (D = 21 nm ± 3.1 nm) was determined by TEM. Magnetic properties of PS-CoNPs were measured using VSM at room temperature: M_s = 35.1 emu/g, H_c = 16100 A/m (202 Oe).

Preparation of PS-CoNPs Using Amine End-Functionalized Polystyrene Surfactant, PS-NH_2 (3). To an oven-dried 100 mL three-neck round-bottom flask equipped with a stir bar and condenser was added PS-NH_2 (**3**, 0.200 g, 4.17×10^{-2} mmol). Solids were dissolved in DCB (20 mL), and the solution was heated to 175 °C. Separately, $Co_2(CO)_8$ (0.300 g, 8.77×10^{-4} mol) was dissolved in DCB (4 mL) at room temperature in air and was rapidly injected into the hot polymer solution. The heating protocols followed were identical to those discussed previously. PS-CoNPs were purified by precipitation into hexanes (500 mL), yielding a black powder (yield = 240 mg). The particle size of the PS-CoNPs (D = 21 nm ± 2.9 nm) was determined using TEM. Magnetic properties of PS-CoNPs were measured using VSM at room temperature: M_s = 34.0 emu/g, H_c = 20700 A/m (260 Oe).

Preparation of PS-CoNPs on 820-mg Scale. To an oven-dried 500 mL three-neck round-bottom flask equipped with a stir bar and condenser was added PS-NH_2 (**3**, 0.800 g, 1.66×10^{-4} mol). Solids were dissolved in DCB (80 mL), and the solution was heated to 175 °C. Separately, $Co_2(CO)_8$ (1.20 g, 3.50×10^{-3} mol) was dissolved in DCB (16 mL) at room temperature in air and was rapidly injected into the hot polymer solution. The heating protocols followed were identical to those for the small-scale model reaction discussed previously. PS-CoNPs were purified by precipitation into hexanes (1000 mL), yielding a black powder (yield = 820 mg). The particle size of the PS-CoNPs (D = 19 nm ± 3.3 nm) was determined using TEM. Magnetic properties of PS-CoNPs were measured using VSM at room temperature: M_s = 41.2 emu/g; H_c = 26300 A/m (330 Oe).

Deposition of PS-CoNPs Dispersions onto a Carbon-Coated TEM Grid (300 Mesh) Exhibiting a Variety of Morphologies. As depicted in Figure 7a,b, PS-CoNPs (D = 21 nm ± 3 nm) were prepared using PS-NH_2 (**3**, M_n = 4800 g/mol) in the thermolysis of $Co_2(CO)_8$. The as-prepared ferrofluid (0.5 mL) was diluted in toluene (10 mL) to yield a PS-CoNPs dispersion (c = 0.5 mg/mL), a drop of which was deposited onto a carbon-coated copper grid and dried in air.

As depicted in Figure 7c,d, PS-CoNPs (D = 21 nm ± 2.9 nm) were prepared using PS-NH_2 (**3**, M_n = 4800 g/mol) in the thermolysis of $Co_2(CO)_8$. The as-prepared ferrofluid (0.5 mL) were diluted into DCB (10.0 mL) to yield a PS-CoNPs dispersion (c = 0.5 mg/mL). A drop of which was deposited onto a carbon-coated copper grid and allowed to slowly evaporate in air under an applied magnetic field (100 mT).

As depicted in Figure 7e,f, PS-CoNPs (D = 21 nm ± 3.3 nm) were prepared using PS-NH_2 (**3**, M_n = 12000 g/mol) in the thermolysis of $Co_2(CO)_8$. The as-prepared ferrofluid (0.5 mL) was diluted in chlorobenzene (10 mL) to yield a PS-CoNPs dispersion (c = 0.5 mg/mL), a drop of which was deposited onto a carbon-coated copper grid and dried in air.

As depicted in Figure 7g,h, PS-CoNPs (D = 21 nm ± 2.9 nm) were prepared using PS-NH_2 (**3**, M_n = 4800 g/mol) in the thermolysis of $Co_2(CO)_8$. The as-prepared ferrofluid (0.5 mL) was diluted in chlorobenzene (10 mL) to yield a PS-CoNPs dispersion (c = 0.5 mg/mL), a drop of which was deposited onto a carbon-coated grid and dried in air.

Acknowledgment. The American Chemical Society Petroleum Research Fund (no. 464I-G10), the Information Storage Industry Consortium (INSIC), the National Science Foundation (J.P., DMR0645618), and the Polymers Division at NIST are gratefully acknowledged for financial support of this research.

REFERENCES AND NOTES

1. Furst, E. M.; Suzuki, C.; Fermigier, M.; Gast, A. P. Permanently Linked Monodisperse Paramagnetic Chains. *Langmuir* **1998**, *14*, 7334–7336.
2. Furst, E. M.; Gast, A. P. Micromechanics of Dipolar Chains Using Optical Tweezers. *Phys. Rev. Lett.* **1999**, *82*, 4130–4133.
3. Sun, S.; Murray, C. B.; Weller, D.; Folks, L.; Moser, A. Monodisperse FePt Nanoparticles and Ferromagnetic FePt Nanocrystal Superlattices. *Science* **2000**, *287*, 1989–1992.
4. Cohen-Tannoudji, L.; Bertrand, E.; Bressy, L.; Goubault, C.; Baudry, J.; Klein, J.; Joanny, J.-F.; Bibette, J. Polymer Bridging Probed by Magnetic Colloids. *Phys. Rev. Lett.* **2005**, *94*, 038301/1038301/4.
5. Goubault, C.; Leal-Calderon, F.; Viovy, J.-L.; Bibette, J. Self-Assembled Magnetic Nanowires Made Irreversible by Polymer Bridging. *Langmuir* **2005**, *21*, 3725–3729.
6. Singh, H.; Laibinis, P. E.; Hatton, T. A. Synthesis of Flexible Magnetic Nanowires of Permanently Linked Core-Shell Magnetic Beads Tethered to a Glass Surface Patterned by Microcontact Printing. *Nano Lett.* **2005**, *5*, 2149–2154.
7. Singh, H.; Laibinis, P. E.; Hatton, T. A. Rigid, Superparamagnetic Chains of Permanently Linked Beads Coated with Magnetic Nanoparticles. Synthesis and Rotational Dynamics under Applied Magnetic Fields. *Langmuir* **2005**, *21*, 11500–11509.
8. Singh, H.; Hatton, T. A. Orientational Dependence of Apparent Magnetic Susceptibilities of Superparamagnetic Nanoparticles in Planar Structured Arrays: Effect on Magnetic Moments of Nanoparticle-Coated Core-Shell Magnetic Beads. *J. Magn. Magn. Mater.* **2007**, *315*, 53–64.
9. Tang, Z.; Kotov, N.A. One-Dimensional Assemblies of Nanoparticles: Preparation, Properties, and Promise. *Adv. Mater.* **2005**, *17*, 951–962.

10. Thomas, J. R. Preparation and Magnetic Properties of Colloidal Cobalt Particles. *J. Appl. Phys.* **1966**, *37*, 2914–2915.
11. de Gennes, P. G.; Pincus, P. A. Pair Correlations in a Ferromagnetic Colloid. *Phys. Kondens. Mater.* **1970**, *11*, 189–198.
12. Griffiths, C. H.; O'Horo, M. P.; Smith, T. W. The Structure, Magnetic Characterization and Oxidation of Colloidal Iron Dispersion. *J. Appl. Phys.* **1979**, *50*, 7108–7115.
13. Chantrell, R. W.; Bradbury, A.; Popplewell, J.; Charles, S. W. Particle Cluster Configuration in Magnetic Fluids. *J. Phys. D: Appl. Phys.* **1980**, *13*, L119–L122.
14. Chantrell, R. W.; Bradbury, A.; Popplewell, J.; Charles, S. W. Agglomerate Formation in a Magnetic Fluid. *J. Appl. Phys.* **1982**, *53*, 2742–2744.
15. Cheng, G.; Romero, D.; Fraser, G. T.; Hight Walker, A. R. Magnetic-Field-Induced Assemblies of Cobalt Nanoparticles. *Langmuir* **2005**, *21*, 12055–12059.
16. Gao, J.; Zhang, B.; Zhang, X.; Xu, B. Magnetic-Dipolar-Interaction-Induced Self- Assembly Affords Wires of Hollow Nanocrystals of Cobalt Selenide. *Angew. Chem., Int. Ed.* **2006**, *45*, 1220–1223.
17. Tripp, S. L.; Puzstay, S. V.; Ribbe, A. E.; Wei, A. Self-Assembly of Cobalt Nanoparticle Rings. *J. Am. Chem. Soc.* **2002**, *124*, 7914–7915.
18. Tripp, S. L.; Dunin-Borkowski, R. E.; Wei, A. Flux-Closure in Self-Assembled Cobalt Nanoparticle Rings. *Angew. Chem., Int. Ed.* **2003**, *42*, 5591–5593.
19. Xiong, Y.; Ye, J.; Gu, X.; Chen, Q. Synthesis and Assembly of Magnetite Nanocubes into Flux-Closure Rings. *J. Phys. Chem. B* **2007**, *111*, 6998–7003.
20. Chen, M.; Liu, J. P.; Sun, S. One-Step Synthesis of FePt Nanoparticles with Tunable Size. *J. Am. Chem. Soc.* **2004**, *126*, 8394–8395.
21. Farrell, D.; Cheng, Y.; Ding, Y.; Yamamuro, S.; Sanchez-Hanke, C.; Kao, C.; Majetich, S. A. Dipolar Interactions and Structural Coherence in Iron Nanoparticle Arrays. *J. Magn. Magn. Mater.* **2004**, *282*, 1–5.
22. Farrell, D.; Cheng, Y.; McCallum, R. W.; Sachan, M.; Majetich, S. A. Magnetic Interactions of Iron Nanoparticles in Arrays and Dilute Dispersions. *J. Phys. Chem. B* **2005**, *109*, 13409–13419.
23. Farrell, D.; Ding, Y.; Majetich, S. A.; Sanchez-Hanke, C.; Kao, C. Structural Ordering Effects in Fe Nanoparticle Two- and Three-Dimensional Arrays. *J. Appl. Phys.* **2004**, *95*, 6636–6638.
24. Goa, Y.; Bao, H.; Beerman, M.; Yasuhara, A.; Shindo, D.; Krishnan, K. Superstructures of Self-assembled Cobalt Nanocrystals. *Appl. Phys. Lett.* **2004**, *84*, 3361.
25. Puntes, V. F.; Gorostiza, P.; Aruguete, D. M.; Bastus, N. G.; Alivisatos, A. P. Collective Behavior in Two-Dimensional Cobalt Nanoparticle Assemblies Observed by Magnetic Force Microscopy. *Nat. Mater.* **2004**, *3*, 263–268.
26. Sun, S.; Murray, C. B. Synthesis of Monodisperse Cobalt Nanocrystals and their Assembly into Magnetic Superlattices. *J. Appl. Phys.* **1999**, *85*, 4325–4330.
27. Hilgendorff, M.; Tesche, B.; Giersig, M. Creation of 3-D Crystals from Single Cobalt Nanoparticles in External Magnetic Fields. *Aust. J. Chem.* **2001**, *54*, 497–501.
28. Pileni, M.-P. Magnetic Fluids: Fabrication, Magnetic Properties, and Organization of Nanocrystals. *Adv. Funct. Mater.* **2001**, *11*, 323–336.
29. Pileni, M. P. Nanocrystal Self-Assemblies: Fabrication and Collective Properties. *J. Phys. Chem. B* **2001**, *105*, 3358–3371.
30. Lalatonne, Y.; Motte, L.; Russier, V.; Ngo, A. T.; Bonville, P.; Pileni, M. P. Mesoscopic Structures of Nanocrystals: Collective Magnetic Properties Due to the Alignment of Nanocrystals. *J. Phys. Chem. B* **2004**, *108*, 1848–1854.
31. Lalatonne, Y.; Richardi, J.; Pileni, M. P. Van der Waals Versus Dipolar Forces Controlling Mesoscopic Organizations of Magnetic Nanocrystals. *Nat. Mater.* **2004**, *3*, 121–125.
32. Giersig, M.; Hilgendorff, M. Magnetic Nanoparticle Superstructures. *Eur. J. Inorg. Chem.* **2005**, 3571–3583.
33. Pileni, M. P. Self-Assembly of Inorganic Nanocrystals: Fabrication and Collective Intrinsic Properties. *Acc. Chem. Res.* **2007**, *40*, 685–693.
34. Shen, L.; Stachowiak, A.; Fateen, S.-E. K.; Hatton, T. A. Structure of Alkanoic cid Stabilized Magnetic Fluids. A Small-Angle Neutron and Light Scattering Analysis. *Langmuir* **2001**, *17*, 288–299.
35. Butter, K.; Philipse, A. P.; Vroege, G. J. Synthesis and Properties of Iron Ferrofluids. *J. Magn. Magn. Mater.* **2002**, *252*, 1–3.
36. Butter, K.; Bomans, P. H. H.; Frederik, P. M.; Vroege, G. J.; Philipse, A. P. Direct Observation of Dipolar Chains in Iron Ferrofluids by Cryogenic Electron Microscopy. *Nat. Mater.* **2003**, *2*, 88–91.
37. Klokkenburg, M.; Vonk, C.; Claesson, E.; Meeldijk, J.; Erne, B.; Philipse, A. Direct Imaging of Zero-Field Dipolar structures in Colloidal Dispersions of Synthetic Magnetite. *J. Am. Chem. Soc.* **2004**, *126*, 16706–16707.
38. Benkoski, J. J.; Bowles, S. E.; Korth, B. D.; Jones, R. L.; Douglas, J. F.; Karim, A.; Pyun, J. Field Induced Formation of Mesoscopic Polymer Chains from Functional Ferromagnetic Colloids. *J. Am. Chem. Soc.* **2007**, *129*, 6291–6297.
39. Benkoski, J. J.; Jones, R. L.; Douglas, J. F.; Karim, A. Photocurable Oil/Water Interfaces as a Universal Platform for 2-D Self-Assembly. *Langmuir* **2007**, *23*, 3530–3537.
40. Hyeon, T. Chemical Synthesis of Magnetic Nanoparticles. *Chem. Commun.* **2003**, 927–934.
41. Lu, A.-H.; Salabas, E. L.; Schüth, F. Magnetic Nanoparticles: Synthesis, Protection, Functionalization and Application. *Angew. Chem., Int. Ed.* **2007**, *46*, 1222–1224.
42. Leslie-Pelecky, D. L.; Rieke, R. D. Magnetic Properties of Nanostructured Materials. *Chem. Mater.* **1996**, *8*, 1770–1783.
43. Pyun, J. Nanocomposite Materials from Functional Polymers and Magnetic Colloids. *Polym. Rev.* **2007**, *47*, 231–263.
44. Burke, N. A. D.; Stöver, H. D. H.; Dawson, F. R. Magnetic Nanocomposites: Preparation and Characterization of Polymer-Coated Iron Nanoparticles. *Chem. Mater.* **2002**, *14*, 4752–4761.
45. Grubbs, R. B. Hybrid Metal-Polymer Composites from Functional Block Copolymers. *J. Polym. Sci., Part A: Polym. Chem.* **2005**, *43*, 4323–4336.
46. Balazs, A. C.; Emrick, T.; Russell, T. P. Nanoparticle Polymer Composites: Where Two Small Worlds Meet. *Science* **2006**, *314*, 1107–1110.
47. Glogowski, E.; Tangirala, R.; Russell, T. P.; Emrick, T. Functionalization of Nanoparticles for Dispersion in Polymers and Assembly in Fluids. *J. Polym. Sci., Part A: Polym. Chem.* **2006**, *44*, 5076–5086.
48. Grubbs, R. B. Role of Polymer Ligands in Nanoparticle Stabilization. *Polym. Rev.* **2007**, *47*, 197–215.
49. Boal, A. K.; Frankamp, B. L.; Uzun, O.; Tuominen, M. T.; Rotello, V. M. Modulation of Spacing and Magnetic Properties of Iron oxide Nanoparticles through Polymer-Mediated "Bricks and Mortar" Self-Assembly. *Chem. Mater.* **2004**, *16*, 3252–3256.
50. Hong, R.; Fisher, N. O.; Emrick, T.; Rotello, V. M. Surface PEGylation and Ligand Exchange Chemistry of FePt Nanoparticles for Biological Application. *Chem. Mater.* **2005**, *17*, 4617–4621.
51. Frankamp, B. L.; Fischer, N. O.; Hong, R.; Srivastava, S.; Rotello, V. M. Surface Modification using Cubic Silsesquioxane Ligands. Facile Synthesis of Water-Soluble Metal Oxide Nanoparticles. *Chem Mater.* **2006**, *18*, 956–959.
52. Lutz, J.-F.; Stiller, S.; Hoth, A.; Kaufner, L.; Pison, U.; Cartier, R. One-Pot Synthesis of PEGylated Ultra Small Iron-Oxide Nanoparticles and Their in Vivo Evaluation as Magnetic Resonance Imaging Contrast Agents. *Biomacromolecules* **2006**, *7*, 3132–3138.

53. Xie, J.; Xu, C.; Xu, Z.; Hou, Y.; Young, K. L.; Wang, S. X.; Pourmond, N.; Sun, S. Linking Hydrophilic Macromolecules to Monodisperse Magnetite (Fe_3O_4) Nanoparticles via Trichloro-s-triazine. *Chem. Mater.* **2006**, *18*, 5401–5403.
54. Frankamp, B. L.; Boal, A. K.; Tuominen, M. T.; Rotello, V. M. Direct Control of the Magnetic Interaction between Iron Oxide Nanoparticles through Dendrimer-Mediated Self-Assembly. *J. Am. Chem. Soc.* **2005**, *127*, 9731–9735.
55. Kim, B.-S.; Qiu, J.-M.; Wang, J.-P.; Taton, T. A. Magnetomicelles: Composite Nanostructures from Magnetic Nanoparticles and Cross-Linked Amphiphilic Block Copolymers. *Nano Lett.* **2005**, *5*, 1987–1991.
56. Kim, M. S.; Chen, Y. F.; Liu, Y. C.; Peng, X. G. Super-stable, High Quality Fe_3O_4 Dendron-Nanocrystals Dispersible in Both Organics and Aqueous Solutions. *Adv. Mater.* **2005**, *17*, 1429–1432.
57. Vestal, C. R.; Zhang, Z. J. Atom Transfer Radical Polymerization Synthesis and Magnetic Characterization of $MnFe_2O_4$/Polystyrene Core/Shell Nanoparticles. *J. Am. Chem. Soc.* **2002**, *124*, 14312–14313.
58. Matsuno, R.; Yamamoto, K.; Otsuka, H.; Takahara, A. Polystyrene-Grafted Magnetite Nanoparticles Prepared through Surface-Initiated Nitroxyl-Mediated Radical Polymerization. *Chem. Mater.* **2003**, *15*, 3–5.
59. Wang, Y.; Teng, X.; Wang, J.-S.; Yang, H. Solvent-Free Atom Transfer Radical Polymerization in the Synthesis of Fe_2O_3@Polystyrene Core-Shell Nanoparticles. *Nano Lett.* **2003**, *3*, 789–793.
60. Marutani, E.; Yamamoto, S.; Ninjbadgar, T.; Tsujii, Y.; Fukuda, T.; Takano, M. Surface Initiated Atom Transfer Radical Polymerization of Methyl Methacrylate on Magnetite Nanoparticles. *Polymer* **2004**, *45*, 2231–2235.
61. Matsuno, R.; Yamamoto, K.; Otsuka, H.; Takahara, A. Polystyrene- and Poly(3-vinylpyridine)-Grafted Magnetite Nanoparticles Prepared through Surface-Initiated Nitroxide-Mediated Radical Polymerization. *Macromolecules* **2004**, *37*, 2203–2209.
62. Ninjbadgar, T.; Yamamoto, S.; Fukuda, T. Synthesis and Magnetic Properties of y-Fe_2O_3/Poly-(methyl methacrylate)-Core/Shell Nanoparticles. *Solid State Sci.* **2004**, *6*, 879–885.
63. Gravano, S. M.; Dumas, R.; Liu, K.; Patten, T. E. Methods for the Surface Functionalization of γ-Fe_2O_3 Nanoparticles with Initiators for Atom Transfer Radical Polymerization and the Formation of Core–Shell Inorganic–Polymer Structures. *J. Polym. Sci., Part A: Polym. Sci.* **2005**, *43*, 3675–3688.
64. Gelbrich, T. F. M.; Schmidt, A. M. Magnetic Thermoresponsive Core–Shell Nanoparticles. *Macromolecules* **2006**, *39*, 3469–3472.
65. Sun, Y.; Ding, X.; Zheng, Z.; Cheng, X.; Hu, X.; Peng, Y. Magnetic Separation of Polymer Hybrid Iron Oxide Nanoparticles Triggered by Temperature. *Chem. Commun.* **2006**, *26*, 2765–2767.
66. Wakamatsu, H.; Yamamota, K.; Nakao, A.; Aoyagi, T. Preparation and Characterization of Temperature-Responsive Magnetite Nanoparticles Conjugated with N-isopropylacrylamide based Functional Copolymer. *J. Magn. Magn. Mater.* **2006**, *302*, 327–333.
67. Lattuada, M.; Hatton, T. A. Functionalization of Monodisperse Magnetic Nanoparticles. *Langmuir* **2007**, *23*, 2158–2168.
68. Hess, P. H.; Parker, P. H. Polymers for Stabilization of Colloidal Cobalt Particles. *J. Appl. Polym. Sci.* **1966**, *10*, 1915.
69. Platonova, O. A.; Bronstein, L. M.; Solodovnikov, S. P.; Yanovskaya, I. M.; Obolonkova, E. S.; Valetsky, P. M.; Wenz, E.; Antonietti, M. Polymers for Stabilization of Colloidal Cobalt Particles. *Colloid Polym. Sci.* **1997**, *275*, 426–431.
70. Rutnakornpituk, M.; Thompson, M. S.; Harris, L. A.; Farmer, K. E.; Esker, A. R.; Riffle, J. S.; Connolly, J.; Pierre, T. G. Formation of Cobalt Nanoparticle Dispersions in the Presence of Polysiloxane Block Copolymers. *Polymer* **2002**, *43*, 2337–2348.
71. Tadd, E.; Bradley, J.; Tannenbaum, R. Spatial Distribution of Cobalt Nanoclusters in Block Copolymers. *Langmuir* **2002**, *18*, 2378–2384.
72. Diana, F. S.; Lee, S.-H.; Petroff, P. M.; Kramer, E. J. Fabrication of hcp-Co Nanocrystals via Rapid Pyrolysis in Inverse PS-b-PVP Micelles and Thermal Annealing. *Nano Lett.* **2003**, *3*, 891–895.
73. Liu, G. J.; Yan, X. H.; Curda, C.; Lal, J. One-Pot Synthesis of Block Copolymer Coated Cobalt Nanocrystals. *Chem. Mater.* **2005**, *17*, 4985–4991.
74. Puntes, V. F.; Krishnan, K. M.; Alivisatos, A. P. Colloidal Nanocrystal Shape and Size Control: The Case of Cobalt. *Science* **2001**, *291*, 2115–2117.
75. Puntes, V. F.; Zanchet, D.; Erdonmez, C. K.; Alivisatos, A. P. Synthesis of hcp Co Nanodisks. *J. Am. Chem. Soc.* **2002**, *124*, 12874–12880.
76. Korth, B. D.; Keng, P.; Shim, I.; Bowles, S. E.; Tang, C.; Kowalewski, T.; Nebesny, K. W.; Pyun, J. Polymer Coated Ferromagnetic Colloids from Well-Defined Macromolecular Surfactants and Assembly into Nanoparticle Chains. *J. Am. Chem. Soc.* **2006**, *128*, 6562–6563.
77. Hawker, C. J.; Bosman, A. W.; Harth, E. New Polymer Synthesis by Nitroxide Mediated Living Radical Polymerizations. *Chem. Rev.* **2001**, *101*, 3661–3688.
78. Lacroix-Desmazes, P.; Lutz, J. F.; Chauvin, F.; Severac, R.; Boutevin, B. Living Radical Polymerization: Use of an Excess of Nitroxide as a Rate Moderator. *Macromolecules* **2001**, *34*, 8866–8871.
79. Matyjaszewski, K.; Xia, J. Atom Transfer Radical Polymerization. *Chem. Rev.* **2001**, *101*, 2921–2990.
80. Ing, H. R.; Manske, R. H. F. Modification of the Gabriel Synthesis of Amines. *J. Am. Chem. Soc.* **1926**, *48*, 2348–2351.
81. Williams, R. H.; Hamilton, L. A. Di-*n*-alkylphosphine Oxides. I. Synthesis. *J. Am. Chem. Soc.* **1952**, *74*, 5418–5419.
82. Skaff, H.; Ilker, M. F.; Coughlin, E. B.; Emrick, T. Preparation of Cadmium Selenide–Polyolefin Composites from Functional Phosphine Oxides and Ruthenium-Based Metathesis. *J. Am. Chem. Soc.* **2002**, *124*, 5729–5733.
83. Witt, D.; Rachon, J. Reactivity of $>$P-O$^-$ Nucleophiles Toward Arylmethyl Chloride Systems. *Heteroatom Chem.* **1999**, *5*, 434–439.
84. Pascual, S.; Coutin, B.; Tardi, M.; Polton, A.; Vairon, J. P. Homogeneous ATRP of Styrene initiated by 1-chloro-1-phenylethane/Copper(I) Chloride/Bipyridine in the Presence of DMF. *Macromolecules* **1999**, *32*, 1432–1437.
85. Samia, A.; Hyzer, K.; Schlueter, J.; Qin, C.-J.; Jiang, S.; Bader, S.; Lin, X.-M. Ligand Effect on the Growth and Digestion of Co Nanocrystals. *J. Am. Chem. Soc.* **2005**, *127*, G126–4126.
86. Weis, J. J. Simulation of Quasi-Two-Dimensional Dipolar Systems. *J. Phys.: Condens. Matter.* **2003**, *15*, S1471–S1495.
87. Diehl, M. R.; Yu, J.-Y.; Heath, J. R.; Held, G. A.; Doyle, H.; Sun, S.; Murray, C. B. Crystalline, Shape, and Surface Anisotropy in Two Crystal Morphologies of Superparamagnetic Cobalt Nanoparticles by Ferromagnetic Resonance. *J. Phys. Chem. B* **2001**, *105*, 7913–7919.
88. Bao, Y.; Beerman, M.; Krishnan, K. M. Controlled Self Assembly of Colloidal Cobalt Nanocrystals. *J. Magn. Magn. Mater.* **2003**, *266*, L245–L249.
89. Dinega, D. P.; Bawendi, M. G. A Solution-Phase Approach to a New Crystal Structure of Cobalt. *Angew. Chem., Int. Ed.* **1999**, *38*, 1788–1791.
90. Sun, S.; Murray, C. B. Synthesis of Monodisperse Cobalt Nanocrystals and Their Assembly into Magnetic Superlattices. *J. Appl. Phys.* **1999**, *85*, 4325–4330.
91. Wei, D.; Patey, G. N. Orientational Order in Simple Dipolar Liquids: Computer Simulation of a Ferroelectric Nematic Phase. *Phys. Rev. Lett.* **1992**, *68*, 2043–2045.
92. Stevens, M. J.; Grest, G. S. Coexistence in Dipolar Fluids in a Field. *Phys. Rev. Lett.* **1994**, *72*, 3686–3689.

93. Stevens, M. J.; Grest, G. S. Phase Coexistence of a Stockmayer Fluid in an Applied Field. *Phys. Rev. E* **1995**, *51*, 5976–5983.
94. Stevens, M. J.; Grest, G. S. Structure of Soft-Sphere Dipolar Fluids. *Phys. Rev. E* **1995**, *51*, 5962–5975.
95. Tlusty, T.; Safran, S. A. Defect-Induced Phase Separation in Dipolar Fluids. *Science* **2000**, *290*, 1328–1331.
96. Stambaugh, J.; Van Workum, K.; Douglas, J. F.; Losert, W. Polymerization Transitions in Two Dimensional Systems of Dipolar Spheres. *Phys. Rev. E* **2005**, *72*, 031301/1031301/4.
97. Van Workum, K.; Douglas, J. F. Equilibrium Polymerization in the Stockmayer Fluid as a Model of Supermolecular Self Organization. *Phys. Rev. E* **2005**, *71*, 031502/1031502/15.
98. Van Workum, K.; Douglas, J. F. Symmetry, Equivalence, and Molecular Self-Assembly. *Phys. Rev. E* **2006**, *73*, 031502/1031502/17.
99. Lavender, H. B.; Iyer, A. K.; Singer, S. J. Global Orientational Order in Model Polar Clusters. *J. Chem. Phys.* **1994**, *101*, 7856–7867.
100. Miller, M. A.; Wales, D. J. Novel Structural Motifs in Clusters of Dipolar Spheres: Knots, Links, and Coils. *J. Phys. Chem. B* **2005**, *109*, 23109–23112.
101. Arshady, R.; Kenner, G. W.; Ledwith, A. The Introduction of Chloromethyl Groups into Styrene-based Polymers. *Makromol. Chem.* **1976**, *177*, 2911–2918.
102. Ryu, S. W.; Hirao, A. Anionic Synthesis of Well-Defined Poly(*m*-halomethylstyrene)s and branched Polymers via Graft-onto Methodology. *Macromolecules* **2000**, *33*, 4765–4771.